

Electronic Supplementary Information

Synergistic effect on ammonia borane hydrolysis by Co catalysts with atomically dispersed CoN_x active sites for hydrogen generation

Pui-Ching Poon^{a†}, Yuanhao Wang^{b†}, Weiqun Li^{c†}, Dawson Wai-Shun Suen^a, William Wai Yan Lam^a, Denise Zi Jing Yap^a, B. Layla Mehdi^c, Jun Qi^d, Xiao-Ying Lu^a, Eugene Yin Cheung Wong^{*b}, Chunzhen Yang^{*d}, Chi-Wing Tsang^{*a}

^a Faculty of Science and Technology, Technological and Higher Education Institute of Hong Kong (THEi), Hong Kong 999077, China

^b Department of Supply Chain and Information Management, The Hang Seng University of Hong Kong, Hong Kong 999077, Hong Kong 999077, China

^c Department of Mechanical, Materials and Aerospace Engineering, University of Liverpool, Liverpool L69 3GQ, United Kingdom

[†] Equal contributions

* To whom correspondence should be addressed: Fax: + 852-2176-1554; E-mail: ctsang@thei.edu.hk; eugenewong@hsu.edu.hk; yangchzh6@mail.sysu.edu.cn

Homepage: <https://www.thei.edu.hk/staff/details/chi-wing-alex-tsang>

A. Experimental Details

A.1 X-ray diffraction

X-ray diffraction (XRD) patterns were recorded on a Rigaku Smartlab instrument, using a Cu K α monochromatized radiation source at 1.54056 Å. Diffraction patterns were collected in ranges of 2 θ from 10°–80° with a step size of 0.02 and a dwell time of 0.25 second per step. The receiving slit (RS), scattering prevention slit (SS) and divergence slit (DS) were 1/2°, 10 mm and 10 mm, respectively.

A.2 Raman spectroscopy

Raman spectra were recorded at room temperature on a HORIBA LabRAM HR Evolution Raman Microscope (manufactured in France SAS) equipped with a liquid-nitrogen cooled multiple detectors including charge coupled device (CCD) detector and a confocal microscope. The line at 532 nm Ar laser was used as an excitation source and the scanning range was 50–3500 nm $^{-1}$. The laser was focused on the sample under a microscope with the diameter of the analysed spot being ~1 μm. The wavenumber values reported were accurate to within 2 cm $^{-1}$.

A.3 X-ray photoelectron spectroscopy

X-ray photoelectron spectra (XPS) were measured using a photoelectron spectrometer (XPS, PHI 5600) with a monochromatic Al K α X-ray source. The binding energy was preliminarily calibrated using the peak positions of the adventitious carbon (C 1s, 284.6 eV). The composition of Co oxidation states was estimated by the deconvolution of Co 3d doublet. Relative element concentrations of N and C were determined by the integral areas of the core-level spectra. After the background was subtracted according to the Shirley method, the spectra were fitted into several peaks using a convolution of Gaussian and Lorentzian functions.

A.4 Scanning electron microscope

Scanning electron microscope (SEM) morphological images of the catalyst samples were obtained on a FE-SEM (Hitachi S-4800) electron microscope with a voltage range of 0.5–30 kV.

A.5 Transmission electron microscopy

The microstructure and element distributions were carried out using transmission electron microscope (TEM, JEM2100+, JEOL) operated at 200 keV. The Co/CoN_x-CNT sample particles were ground between two glass slides, and dispersed on the copper grid.

A.6 Specific surface area measurement (BET)

The specific surface areas and pore size distributions of catalysts samples were analyzed at liquid nitrogen temperature by the Brunauer–Emmett–Teller (BET) and Barrett-Joyner-Halenda (BJH) methods (Micromeritics, ASAP2020). The samples were degassed with a vacuum at 350°C for 12 hours before conducting nitrogen adsorption-desorption isotherm at liquid nitrogen temperature.

A.7 X-ray absorption spectroscopy measurement (XAS)

The X-ray absorption fine structure (XAFS) measurement was performed at BL11B1 beamline of Shanghai Synchrotron Radiation Facility (SSRF) operated at 3.5 GeV under “top-up” mode with a constant current of 200 mA. The photon energy was adjusted near 7709 eV for the Co K-edge measurement. XAFS data were recorded under fluorescence mode using a Lytle detector which was shielded by a Fe filter. The Co foil X-ray energy was used to calibrate the absorption edge for all Co catalysts. XAFS data analyses was conducted using Athena and Artemis software.

B. List of figures:

Fig. S1 X-ray diffraction patterns of the Co/Co SACs catalyst with nominal ratio (Co: DCD-350 = 1:33.3) calcined at various carbonization temperatures.....	5
Fig. S2 (a, b) FE-SEM image of the Co/Co SACs catalyst after used for 15 cycles.....	5
Fig. S3 X-ray diffraction pattern of the Co/CoN _x -CNT-33-800T catalyst with nominal ratio of Co: DCD-350 = 1:33.3 after used for 15 cycles.....	5
Fig. S4 Raman spectrum of the Co/CoN _x -CNT-33-800T catalyst with nominal ratio of Co: DCD-350 = 1:33.3 after used for 15 cycles.	6
Fig. S5 XPS survey of the as-prepared Co/CoN _x -CNT-33-800T catalyst with nominal ratio of Co: DCD-350 = 1:33.3 carbonized at 800°C.	6
Fig. S6 Comparison of the high resolution XPS spectra: (a) Co/CoN _x -CNT-33-800T; (b) Co phthalocyanine; (c) Co nanoparticles.....	7
Fig. S7 (a) Yield of carbonized catalytic materials starting from 5 g of DCD-350 with various Co:DCD-350 ratio: (i) Co/CoN _x -CNT-33-800T (yield: 0.44 g); (ii) Co/CoN _x -CNT-40-800T (yield: 0.28 g); (iii) Co/CoN _x -CNT-50-800T (yield: 0.18 g); (iv) Co/CoN _x -CNT-66-800T (yield: 0.07 g); (v) Co/CoN _x -CNT-100-800T (yield: 0.70 g); (vi) Co/CoN _x -CNT-125-800T (yield: 0.12 g); (vii) Co/CoN _x -CNT-166-800T (yield: 0.09 g); (viii) Co/CoN _x -CNT-250-800T (yield: 0.05 g); (b) Catalytic performances (TOF) of the Co/Co-N-CNT catalysts at various Co:DCD-350 ratio and the corresponding synthetic yield from 5 g of DCD-350 materials; (c) the corresponding specific hydrogen generation rate.....	8
Fig. S8 Catalytic performance under limited amount of water volume. Test conditions: 0.04 g of Co/CoN _x -CNT-33-800T catalyst (Co: DCD-350 = 1:33.3), 0.04 g of ammonia borane and 1 mL of water.	9
Fig. S9 N ₂ adsorption isotherm of the after-acid-leached Co/CoNx-CNT at 77 K (black and red lines represent adsorption and desorption branches, respectively; (b) mesopore size distribution determined from Barrett-Joyner-Halenda (BJH) method of the leached material.	9
Fig. S10 High resolution XPS spectra of the Co/CoN _x -CNT-33-800T catalyst after 5 times of uses: (a) C 1s; (b) Co 2p; (c) N 1s; (d) O 1s.....	10
Fig. S11 Comparison of the XANES (a) and EXAFS (b) spectra of Co/CoN _x -CNT-33-800T at Co K-edge before and after catalysis reaction. Arrows indicate the changes in the spectra between the pristine and treated samples.	10

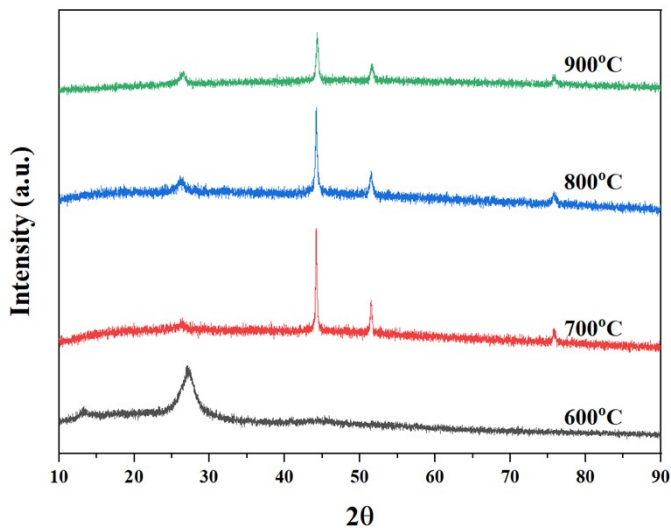


Fig. S1 X-ray diffraction patterns of the Co/Co SACs catalyst with nominal ratio (Co: DCD-350 = 1:33.3) calcined at various carbonization temperatures.

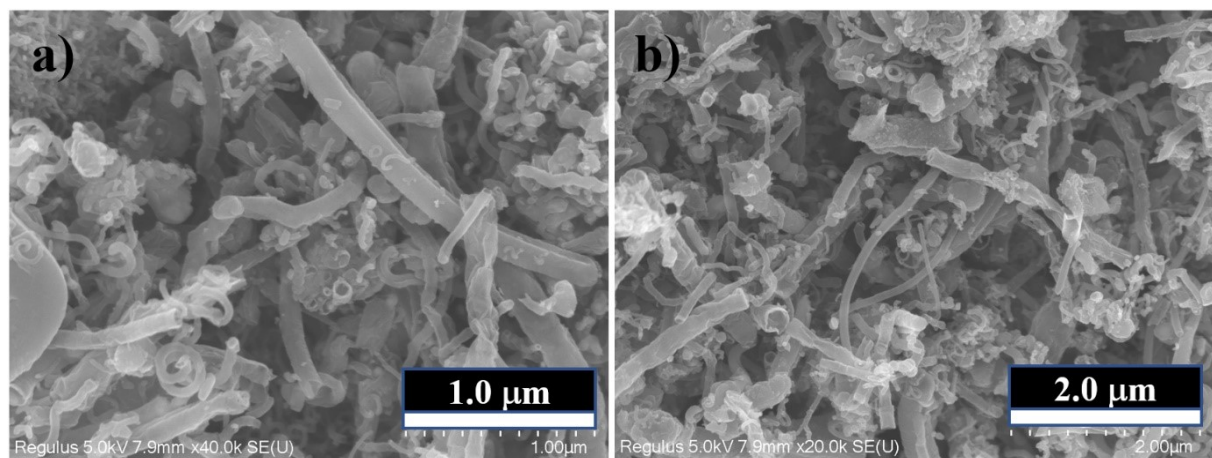


Fig. S2 (a, b) FE-SEM image of the Co/Co SACs catalyst after used for 15 cycles.

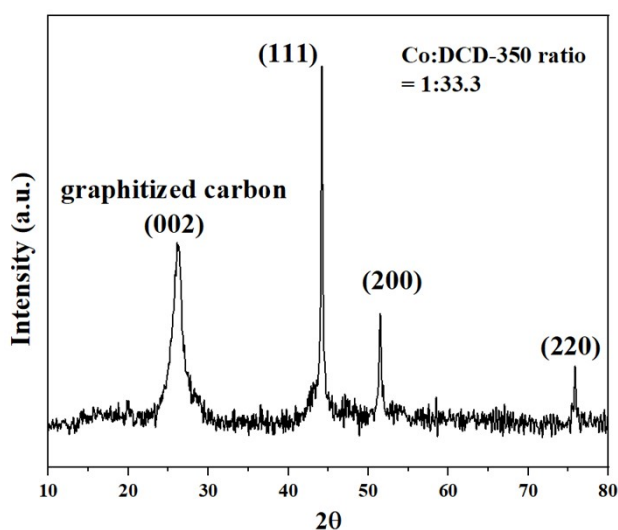


Fig. S3 X-ray diffraction pattern of the Co/CoN_x-CNT-33-800T catalyst with nominal ratio of Co: DCD-350 = 1:33.3 after used for 15 cycles.

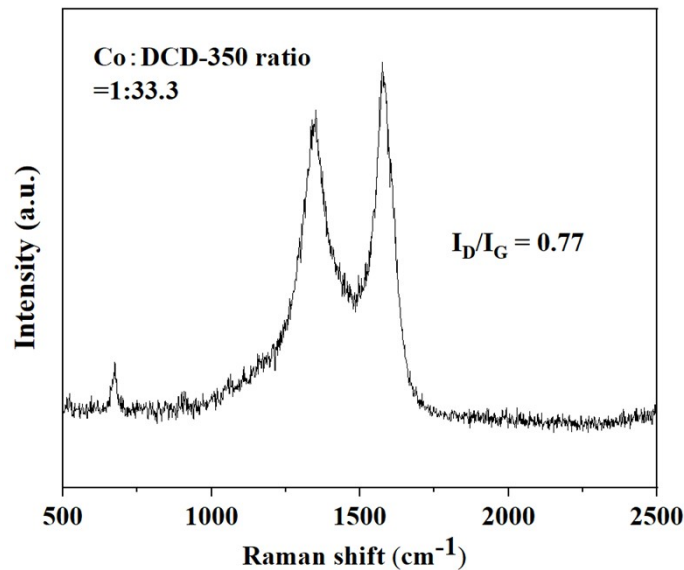


Fig. S4 Raman spectrum of the Co/CoNx-CNT-33-800T catalyst with nominal ratio of Co: DCD-350 = 1:33.3 after used for 15 cycles.

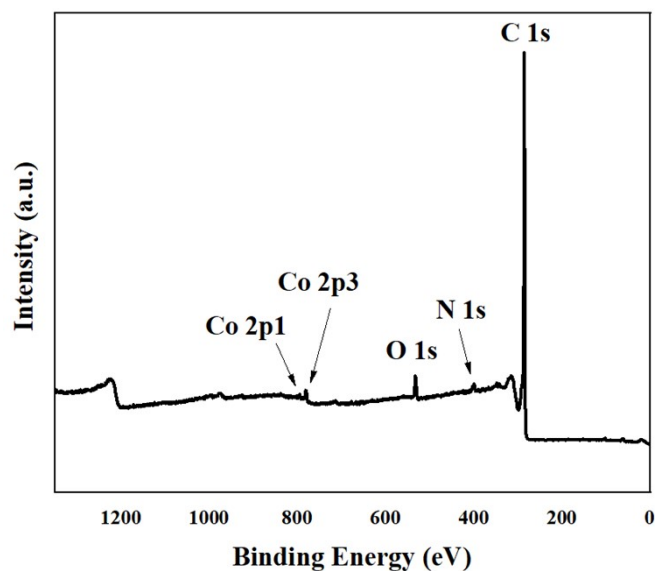


Fig. S5 XPS survey of the as-prepared Co/CoNx-CNT-33-800T catalyst with nominal ratio of Co: DCD-350 = 1:33.3 carbonized at 800°C.

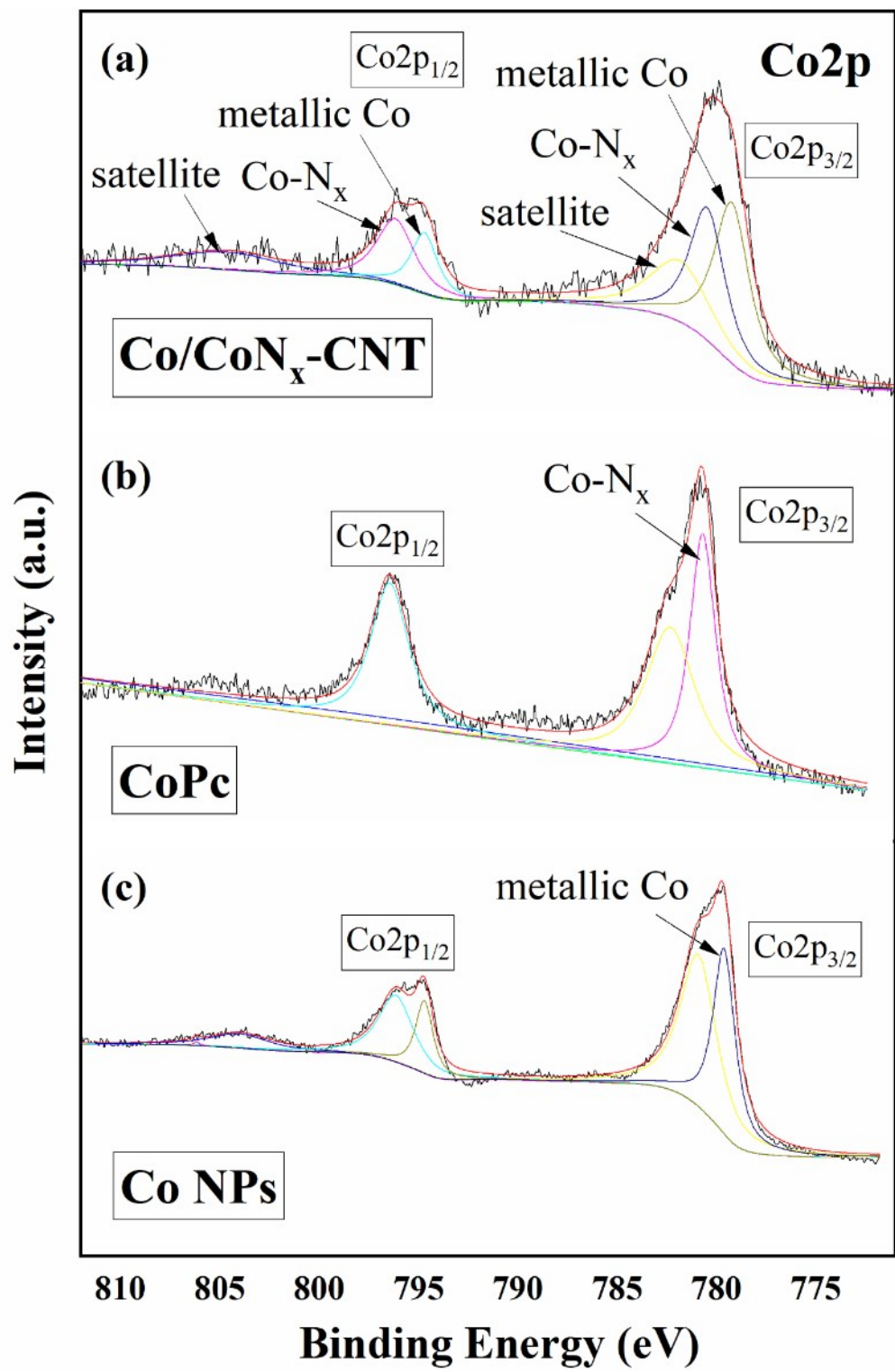


Fig. S6 Comparison of the high resolution XPS spectra: **(a)** Co/CoN_x-CNT-33-800T; **(b)** Co phthalocyanine; **(c)** Co nanoparticles.

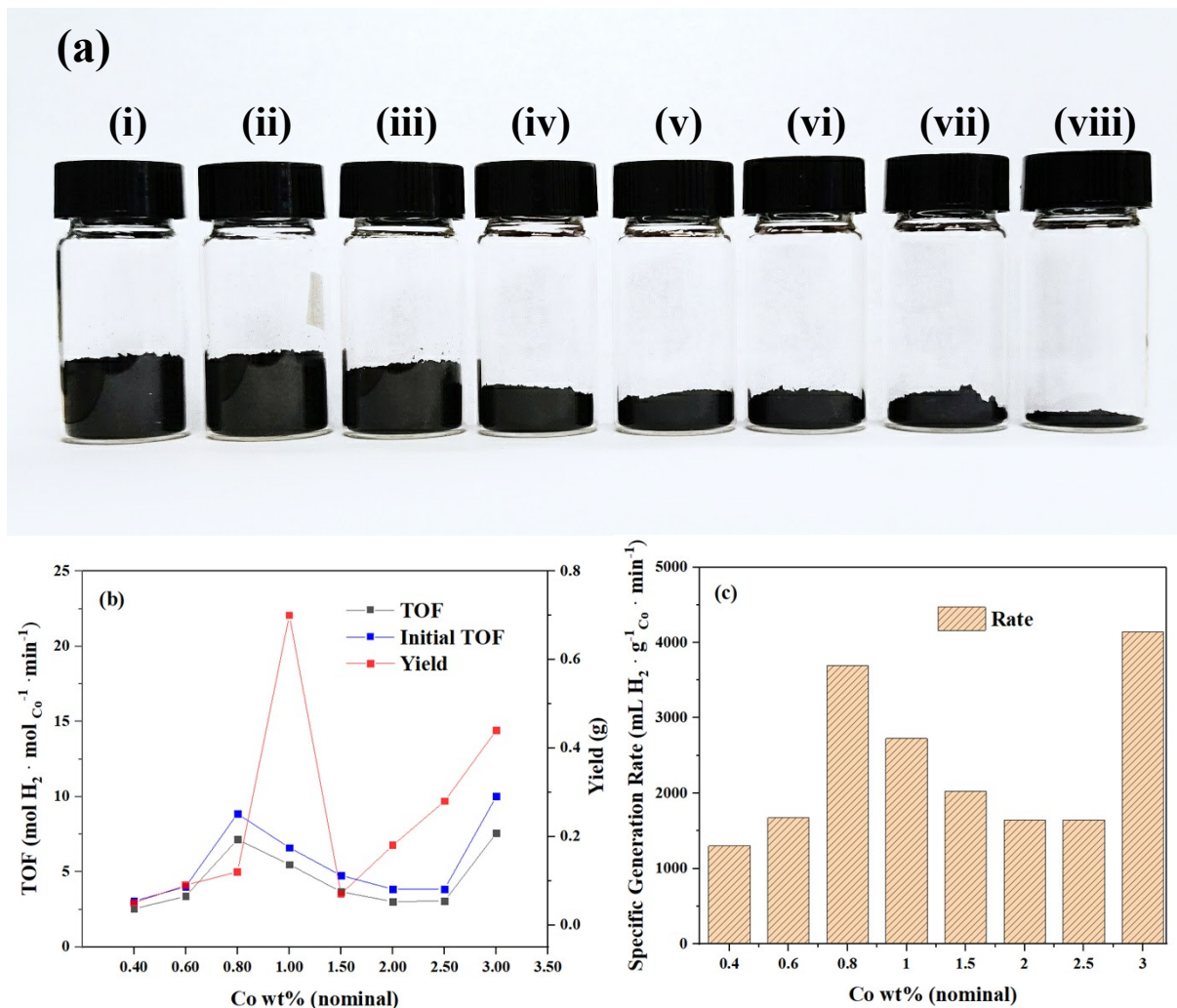


Fig. S7 (a) Yield of carbonized catalytic materials starting from 5 g of DCD-350 with various Co:DCD-350 ratio: (i) Co/CoN_x-CNT-33-800T (yield: 0.44 g); (ii) Co/CoN_x-CNT-40-800T (yield: 0.28 g); (iii) Co/CoN_x-CNT-50-800T (yield: 0.18 g); (iv) Co/CoN_x-CNT-66-800T (yield: 0.07 g); (v) Co/CoN_x-CNT-100-800T (yield: 0.70 g); (vi) Co/CoN_x-CNT-125-800T (yield: 0.12 g); (vii) Co/CoN_x-CNT-166-800T (yield: 0.09 g); (viii) Co/CoN_x-CNT-250-800T (yield: 0.05 g); (b) Catalytic performances (TOF) of the Co/Co-N-CNT catalysts at various Co:DCD-350 ratio and the corresponding synthetic yield from 5 g of DCD-350 materials; (c) the corresponding specific hydrogen generation rate.

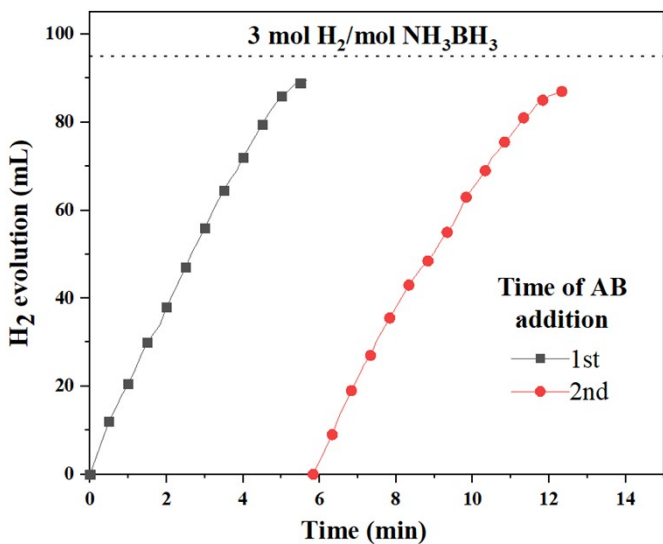


Fig. S8 Catalytic performance under limited amount of water volume. Test conditions: 0.04 g of Co/CoN_x-CNT-33-800T catalyst (Co: DCD-350 = 1:33.3), 0.04 g of ammonia borane and 1 mL of water.

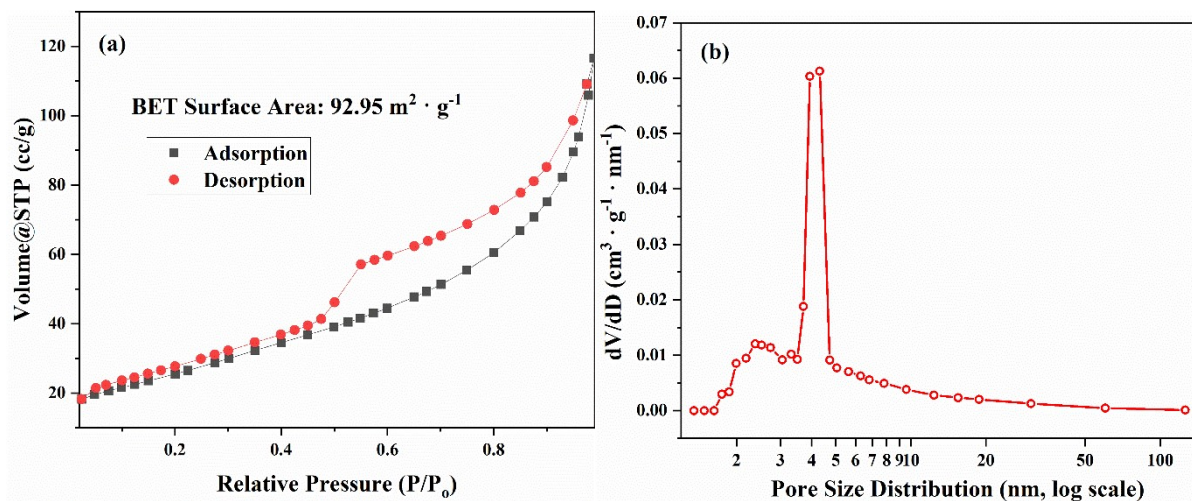


Fig. S9 (a) N₂ adsorption isotherm of the after-acid-leached Co/CoNx-CNT at 77 K (black and red lines represent adsorption and desorption branches, respectively; (b) mesopore size distribution determined from Barrett-Joyner-Halenda (BJH) method of the leached material.

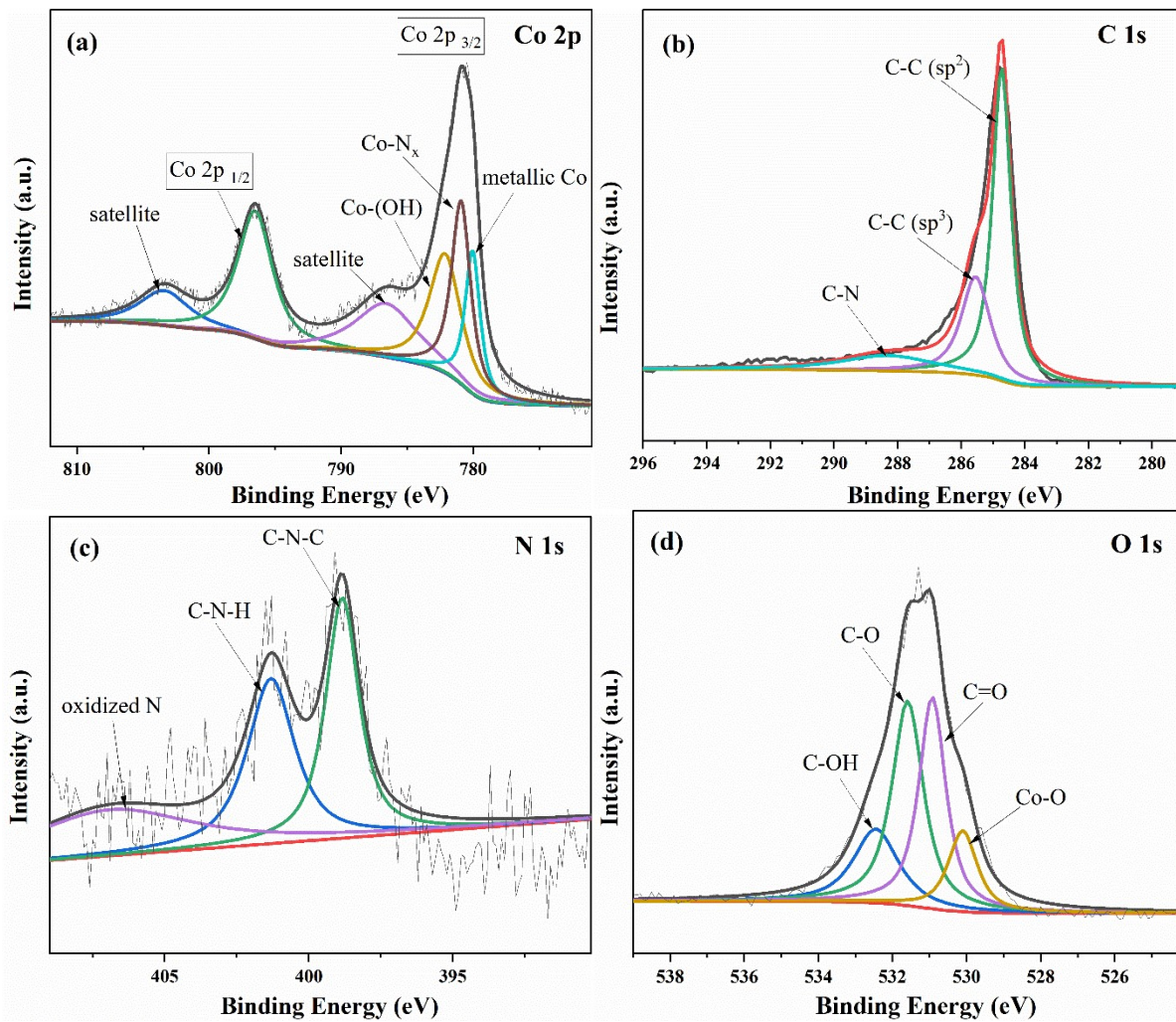


Fig. S10 High resolution XPS spectra of the Co/CoNx-CNT-33-800T catalyst after 5 times of uses: (a) C 1s; (b) Co 2p; (c) N 1s; (d) O 1s.

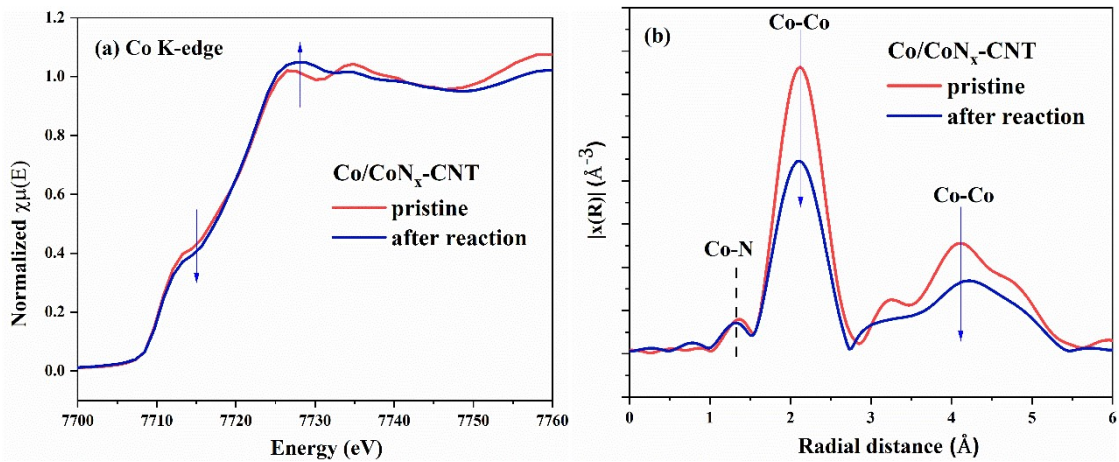


Fig. S11 Comparison of the XANES (a) and EXAFS (b) spectra of Co/CoNx-CNT-33-800T at Co K-edge before and after catalysis reaction. Arrows indicate the changes in the spectra between the pristine and treated samples.

Table S1 Comparison of the TOF values, generation rates and the stability of various Co-based metal catalysts for ammonia borane hydrolysis.

Catalysts	Reaction temp. (°C)	TOF ($mol_{H_2} \cdot mol_{Cat}^{-1}$)	Max specific generation rate (r_B) ($mL_{H_2} \cdot g_{Co}^{-1} \cdot min^{-1}$)	E_a (kJ·mol ⁻¹)	Times of recycling use (th)	Stability (%)	Reference
Co/CoN _x -CNT support	40	13.3	7833	46	40	No observable decay	This work
Co/CoN _x -CNT support	25	2.57	1161	-	-	-	This work
PEI-GO _{3D} /Co	25	18.5	7600	27.41	5	83	¹
Co-Co ₃ O ₄ /CDs	25	17.93	6816	40	5	~50	²
Co-CoO _x @NCS-II	25	13.58	5562	46.37	5	32	³
CoO _x @C-rGO (CCG-i)	30	-	5521	40.57	-	-	⁴
Co-Mo-B/foam sponge	25	-	5100*	41.7	5	62	⁵
Cu _{0.4} Co _{0.6} /BNNFs	25	8.42	3387	21.8	5	55	⁶
Cu _{0.2} Co _{0.8} /HPC	25	-	2960	41.7	4	~33	⁷
Co thin films	25	-	2500	60	6	60	⁸
Co/hydroxyapatite	25	4.54	2200	50	5	81	⁹
Co _{0.52} Cu _{0.48} with starch	25	3.4	2179	37.3	5	66	¹⁰
Pt ₃ Co	25	-	1380	-	-	-	¹¹
Co@g-C ₃ N ₄ -rGO (CNG-I)	25	-	1253	-	-	-	¹²
(Cu _{0.50} Co _{0.50}) ₂ Al-Cat	25	-	1000	-	5	No significant loss of activity	¹³
Co/MIL-101-1-U	25	51.4	-	31.3	30	No significant change	¹⁴

Co@N-C-700	25	5.6	-	31.0	10	97	15
Co@N-C-50	25	12.7**	-	44.9	5	83	16
CuCo@MIL-101	25	19.6	-	-	5	82	17
Co ₃₅ Pd ₆₅ /C	25	22.7	-	27.5	5	75	18
Ag _{0.3} Co _{0.7} @PAMAM/rGO	25	19.79	-	34.21	6	75	19
Silica-embedded cobalt(0)	25	13.2	-	42	5	74	20
Co nanoclusters	25	5.32	-	56	5	69	21
Intrazeolite cobalt(0) nanoclusters	25	5.32	-	56	5	69	21
Co capped by amine	25	39.9	-	28.2	5	66	22
Co-CoO _x @GO-II	25	15.3	-	62.3	5	65	23
Co/graphene	25	13.8	-	32.8	5	60	24
CoNi/graphene	25	16.4	-	13.5	5	25	25
Co/CNT (5wt%)	25	8.5	-	46.9	-	-	26
Co/AC (5wt%)	25	5.8	-	47.2	-	-	26
Co/covalent triazine framework (5wt%)	25	33.5	-	42.7	-	-	26

* At pH = 11

** After activated by NaOH solution

Table S2 Metal contents of catalysts prepared at different weight ratios of Co(acac)₂ to DCD-350.

Co Catalysts Samples	Co wt%
Co/CoN _x -CNT-33-800T	21.9
CoN _x -CNT (after acid leaching of Co/CoN _x -CNT)	10.3
Co/CoN _x -CNT-33-700T	39.2
Co/CoN _x -CNT-33-900T	32.7
Co/CoN _x -CNT-40-800T	26.5
Co/CoN _x -CNT-50-800T	18.5
Co/CoN _x -CNT-66-800T	46.9
Co/CoN _x -CNT-100-800T	54.9
Co/CoN _x -CNT-125-800T	16.9
Co/CoN _x -CNT-166-800T	22.5
Co/CoN _x -CNT-250-800T	31.2

Reference

1. M. Li, J. Hu and H. Lu, *Catal. Sci. Technol.*, 2016, **6**, 7186-7192.
2. H. Wu, M. Wu, B. Wang, X. Yong, Y. Liu, B. Li, B. Liu and S. Lu, *J. Energy Chem.*, 2020, **48**, 43-53.
3. H. Zhang, Y. Fan, B. Liu, Y. Liu, S. Ashraf, X. Wu, G. Han, J. Gao and B. Li, *ACS Sustain. Chem. Eng.*, 2019, **7**, 9782-9792.
4. Y. Liu, H. Guo, K. Sun and J. Jiang, *Int. J. Hydrog. Energy*, 2019, **44**, 28163-28172.
5. C. Li, W. Meng, G. Hu, Y. Wang, Z. Cao and K. Zhang, *Int. J. Hydrog. Energy*, 2018, **43**, 17664-17672.
6. X. Yang, Q. Li, L. Li, J. Lin, X. Yang, C. Yu, Z. Liu, Y. Fang, Y. Huang and C. Tang, *J. Power Sources*, 2019, **431**, 135-143.
7. H. Wang, L. Zhou, M. Han, Z. Tao, F. Cheng and J. Chen, *J. Alloys Compd.*, 2015, **651**, 382-388.
8. M. Paladini, G. M. Arzac, V. Godinho, M. C. J. D. Haro and A. Fernández, *Appl. Catal. B*, 2014, **158-159**, 400-409.
9. M. Rakap and S. Özkar, *Catal. Today*, 2012, **183**, 17-25.
10. W. Sang, C. Wang, X. Zhang, X. Yu, C. Yu, J. Zhao, X. Wang, X. Yang and L. Li, *Int. J. Hydrog. Energy*, 2017, **42**, 30691-30703.
11. C. Yao, L. Zhuang, Y. Cao, X. Ai and H. Yang, *Int. J. Hydrog. Energy*, 2008, **33**, 2462-2467.
12. S. Duan, G. Han, Y. Su, X. Zhang, Y. Liu, X. Wu and B. Li, *Langmuir*, 2016, **32**, 6272-6281.
13. C. Li, J. Zhou, W. Gao, J. Zhao, J. Liu, Y. Zhao, M. Wei, D. G. Evans and X. Duan, *J. Mater. Chem. A*, 2013, **1**, 5370-5376.
14. P. Liu, X. Gu, K. Kang, H. Zhang, J. Cheng and H. Su, *ACS Appl. Mater. Interfaces*, 2017, **9**, 10759-10767.
15. H. Wang, Y. Zhao, F. Cheng, Z. Tao and J. Chen, *Catal. Sci. Technol.*, 2016, **6**, 3443-3448.
16. S. L. Zacho, J. Mielby and S. Kegnæs, *Catal. Sci. Technol.*, 2018, **8**, 4741-4746.
17. J. Li, Q.-L. Zhu and Q. Xu, *Catal. Sci. Technol.*, 2015, **5**, 525-530.
18. D. Sun, V. Mazumder, O. Metin and S. Sun, *ACS Nano*, 2011, **5**, 6458–6464
19. D. Ke, J. Wang, H. Zhang, Y. Li, L. Zhang, X. Zhao and S. Han, *J. Mater. Sci. Technol.*, 2018, **34**, 2350-2358.
20. Ö. Metin, M. Dinç, Z. S. Eren and S. Özkar, *Int. J. Hydrog. Energy*, 2011, **36**, 11528-11535.
21. M. Rakap and S. Özkar, *Int. J. Hydrog. Energy*, 2010, **35**, 3341-3346.
22. J. Hu, Z. Chen, M. Li, X. Zhou and H. Lu, *ACS Appl. Mater. Interfaces*, 2014, **6**, 13191-13200.
23. S. Guan, L. Zhang, H. Zhang, Y. Guo, B. Liu, H. Wen, Y. Fan and B. Li, *Chem.: Asian J.*, 2020, **15**, 3087-3095.
24. L. Yang, N. Cao, C. Du, H. Dai, K. Hu, W. Luo and G. Cheng, *Mater. Lett.*, 2014, **115**, 113-116.
25. W. Feng, L. Yang, N. Cao, C. Du, H. Dai, W. Luo and G. Cheng, *Int. J. Hydrog. Energy*, 2014, **39**, 3371-3380.
26. Z. Li, T. He, L. Liu, W. Chen, M. Zhang, G. Wu and P. Chen, *Chem. Sci.*, 2017, **8**, 781-788.